Lecture Notes in Mechanical Engineering

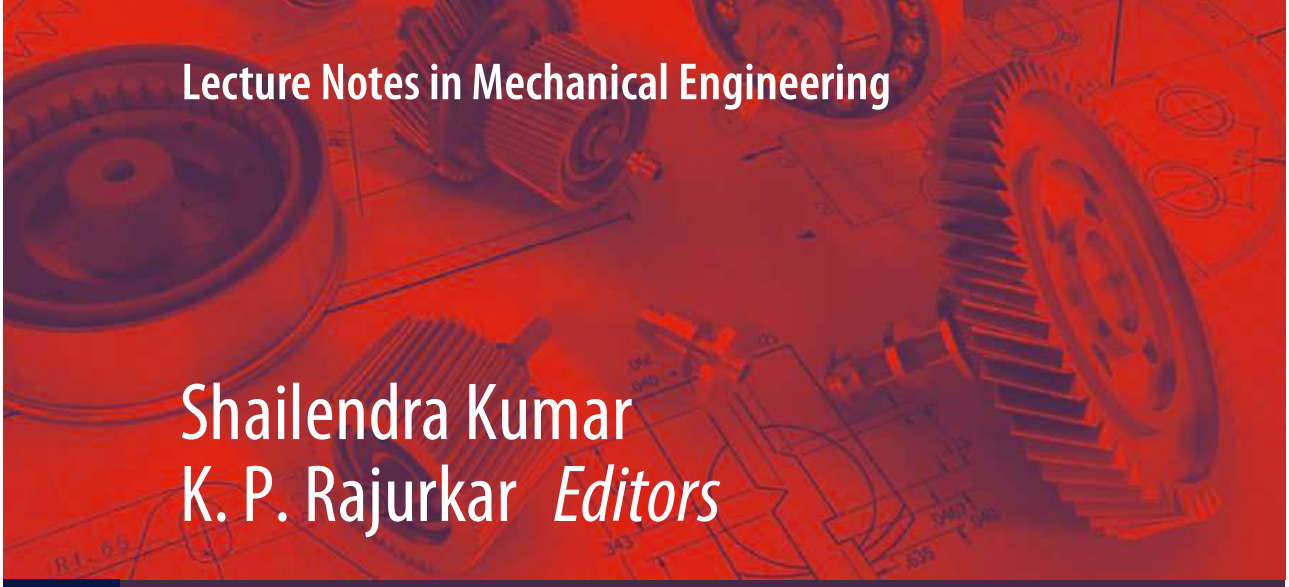

Shailendra Kumar
K. P. Rajurkar *Editors*

Advances in Manufacturing Systems

Select Proceedings of RAM 2020

Springer

Editors
Shailendra Kumar
Sardar Vallabhbhai National Institute of Technology
Surat, India

K. P. Rajurkar
University of Nebraska–Lincoln
Lincoln, OR, USA

ISSN 2195-4356 ISSN 2195-4364 (electronic)
Lecture Notes in Mechanical Engineering
ISBN 978-981-33-4465-5 ISBN 978-981-33-4466-2 (eBook)
https://doi.org/10.1007/978-981-33-4466-2

This Springer imprint is published by the registered company Springer Nature Singapore Pte Ltd.
The registered company address is: 152 Beach Road, #21-01/04 Gateway East, Singapore 189721, Singapore

Contents

Chapter 26
Mechanical and Wear Characterization of Epoxy Resin-Based Functionally Graded Material for Sustainable Utilization of Stone Industry Waste

Aakash Sharma and Vikash Gautam

Introduction

The potential to acknowledge and use materials is essential over time. Due to environmental reasons, many scientists and engineers recognize the importance of using innovative materials. There is always an unceasing growth in the field of materials. Furthermore, the human pursuance to find a new material is never complete by utilizing environmental waste that may work under certain conditions. Significant progress has been made in the development of materials from metals to alloys and functionally graded materials (FGM) based on specific activity. The term "FGM" was coined by the Japanese in 1984 to develop high temperature materials. The idea is to produce a material from a different composition that is resistant to high temperatures on the one hand and good thermal conductivity on the other.

Naebe [1] presented in their article, a review of the latest advances in the investigation of functionally graded materials. The main objective of the research has always been the manufacturing of FGM/C and, therefore, various processing techniques for the preparation of FGM/C are discussed, e.g., CVD, thermal spray, centrifugal casting, electrophoretic deposition, spark plasma sintering, etc. In their articles, Shinohara [2] discussed the challenges of fabricating functionally graded materials and classified its future applications and current issues in various scientific and technological fields, including aerospace, (bio) mechanics, energy engineering, sensor

A. Sharma (✉) · V. Gautam
Department of Mechanical Engineering, Swami Keshvanand Institute of Technology, Jaipur 302025, India
e-mail: aakasharma1507@gmail.com

S. Kumar and K. P. Rajurkar (eds.), *Advances in Manufacturing Systems*,
Lecture Notes in Mechanical Engineering,
https://doi.org/10.1007/978-981-33-4466-2_26

technology and tribology. Researchers also fabricated graded composites using thermoset resins like Ni/Epoxy resin FGM by magnetic field driving method [3], functionally graded porous polymer structure by Thermal bonding lamination technique [4].

FGMs are innovative materials with varying composition. However, there is not much research work done to develop functionally graded materials for Microelectromechanical systems (MEMS) applications. Hasssanin and Jiang [5] discussed a process for fabricating ceramic micro components using the combined properties of Alumina and Zirconia by soft lithography technique. Rezapoor et al. fabricated Fe-TiC functionally graded coating and evaluated its mechanical properties [6]. Salcedo [7] simulated a 3D functionally graded material using material. Gupta and Talha [8] in their review focussed on the recent developments in modeling and simulation techniques of FGM/S. Polajnar and Kalin [9] investigated friction and wear performance of functionally graded ductile iron (FGDI). Fabrication of W-Cu functionally graded materials using spark plasma sintering [10] and its mechanical characterization [11, 12] is also common among researchers.

Techniques of exploiting filler and reinforcement material for the fabrication of functional composites are more common among researchers such as aerosol and coremat filled epoxy composites [13], glass fiber reinforced composite [14], granite epoxy composite with cast iron filler [15], graphite micro filled epoxy composites [16], granite dust filled Polycarbonate (PC) hardened epoxy composite [17], functionally graded aluminium composites using centrifugal casting [18], graded natural fiber/epoxy composite by centrifugal casting using banana trunk as natural fiber [19], granite powder filled epoxy composites [20], marble dust filled epoxy composites [21], granite powder—epoxy composites for chemical resistance testing [22], epoxy resin with flyash particulates as filler [23], polybutylene terepthalate (PBT) toughened epoxy composite [24], granite powder reinforced in toughened epoxy with unsaturated polyester [25], composite filled with glass fiber [26], granite filled composites for wind turbine applications [27, 28], epoxy resin-based ceramic filled composite [29], bamboo/jute—glass fiber-reinforced polymer (GFRP) composite [30], hybrid composites filled with glass fiber and milled carbon [31] etc.

Depending on their behavior, the functional grading of material serves two purposes. The current literature shows that the use of a large number of fillers and fibers in functional grading of polymers are advantageous in enhancing the mechanical as well as wear properties. Waste products from the stone industry, such as granite powder, are widely and prominently exploited in the fabrication of composites. Depending on the background, existing applications focus on the composition of uniform and graduate compounds. Polymer-based granite powder reinforcement homogeneous and FGM samples were examined to determine their mechanical and wear properties.

Materials and Methodology

The standardized composite material is manufactured using a stone industry waste, i.e., granite powder combined with araldite epoxy resin (LY-556) as matrix reinforcing adhesive material. The hardener (HY-917) is used for curing the resin with the composition ratio of 1:10 wt% with epoxy. Granite and epoxy were weighed using an electronic weighing machine and then mixed evenly by hand for about 10 min to remove air bubbles. A mixture of granite and epoxy is carefully found in the glass test tubes 15 mm in diameter and 125 mm long as shown in Fig. 26.1. The composition of granite dust and epoxy is shown in Table 26.1.

Graded samples are produced by vertical centrifugal casting method (Fig. 26.2). First, the glass tubes are coated internally with a wax-releasing agent. The raw material is poured into cylindrical glass tubes with the prescribed weight ratio and rotated for 45 min at 1500 rpm. Prepared samples were left unattended for 48 h at room temperature and then for further testing, extricated from the glass tubes.

Fig. 26.1 Epoxy-granite mixture in glass tube after VCC process

Table 26.1 Material composition

Specimen	Granite dust (%)	Epoxy (%)
A	0	100
B	5	95
C	10	90
D	15	85

Fig. 26.2 Experimental setup for vertical centrifugal casting

Mechanical Characterization

The hardness of the samples was measured using the C-Scale Rockwell Hardness Tester. It was tested by taking initial load of 10 kgf and main load of 150 kgf for dwell time sufficient enough for indentation. Since it is one of the indentation techniques for determining hardness, we used a 120° diamond spheroconical indenter. Figure 26.3 shows indentation marks on the specimens after determining hardness.

A standard sample size of 55 mm × 10 mm is designed for the Charpy impact test rig shown in Fig. 26.4 in accordance with the ASTM E23 standard. Due to the cylindrical shape of the specimens, the anvil had a designed tooling to hold the samples tight enough to withstand the impact of the high potential hammer/pendulum. The energy absorbed by the specimen before fracture can be noted from the energy readout which when divided by cross-section area of the specimen gives us the impact strength.

Sliding Wear Analysis

The wear was tested under dry conditions on the Pin-On-Disc Tribometer (DUCOM) shown in Fig. 26.5a. The experiments were performed according to the factors and levels given in Table 26.2. The test specimens as in Fig. 26.5b required to perform sliding wear analysis were made to a standard size by machining. The sample with diameter 10 mm and length 35 mm were developed as per the requirements of the

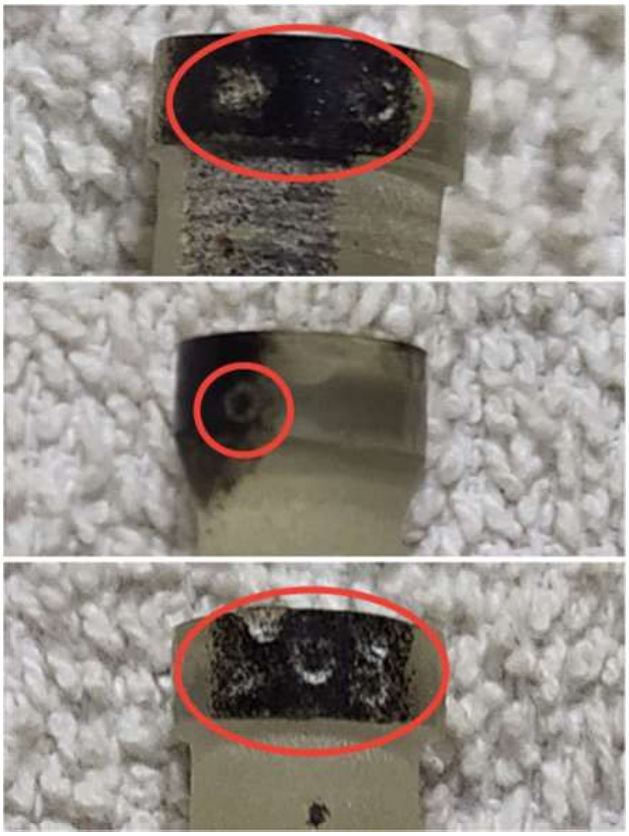

Fig. 26.3 Test specimens for rockwell hardness testing

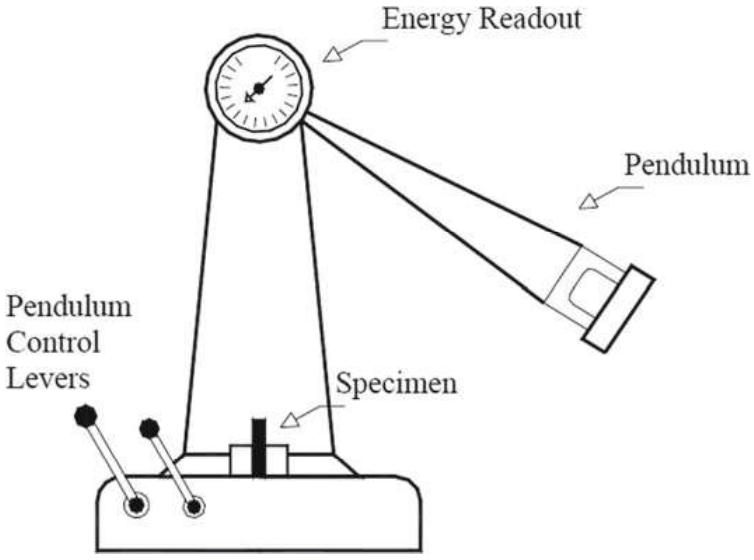

Fig. 26.4 Experimental diagram of charpy impact test

(A)

(B)

Fig. 26.5 **a** Experimental setup of Pin-On-Disc tribometer and **b** Test specimens for sliding wear analysis

Table 26.2 The factors and levels of the experiments

Control factor	Levels				Units
	I	II	III	IV	
Speed	375	750	1125	1500	RPM
Load	7.5	15	22.5	30	Newton
Fiber content	0	5	10	15	%
Distance	150	300	450	600	Meters

Tribometer. The test surface was ground with 400 and 800 high quality SiC abrasive paper to make sure that specimens make proper contact with the steel disc. The sample surfaces were cleaned with soft cotton soaked in acetone after each tribometer run to remove debris caused by wear.

The tests were carried out at different loads, sliding velocities and sliding distances to determine the effect of these variables on the wear rate of compounds produced at a variable proportion of the granite content. The Weighing Electronic Accuracy Machine (WENSAR) is used to measure the mass loss due to wear.

The specific wear rate was analyzed using following equation [21]

$$W_S = \frac{\Delta m}{\rho \times t \times V_S \times F_N}$$

where, W_S is specific wear rate, Δm is mass loss due to wear, ρ is mass per unit volume of the composite, t is the time duration, V_S is the sliding velocity and F_N is average normal load.

Micrographic Observation

Morphological imaging was observed using an LV JEOL JSM-6480 scanning electron microscope. The clean sample was mounted with silver paste on the hole and gold coated under the vacuum in the spray unit for better conductivity before observation. Figures below show the electronic micrograph of granite dust at different magnifications. Granite powder SEM micrographs show that granite powder was fatally present in the group because of the fact that the fabrication method selected was vertical centrifugal casting due to which the powder particles were shown as agglomerates as in Fig. 26.6 and it was also shown that the particles under observation are forked or V-shaped in nature (Fig. 26.7).

Design of Experiment

Taguchi Technology is an optimization tool used to reduce the time required for experiments and determine the impact of effective production parameters. L16 orthogonal imaging was considered in this study to evaluate the performance of material sliding wear and not the mechanical parameters because of the presence of variable factors and levels that is being used in the assessment of specific wear rate of the graded samples [20]. Table 26.3 shows the L_{16} orthogonal array of factors and their DOE notations.

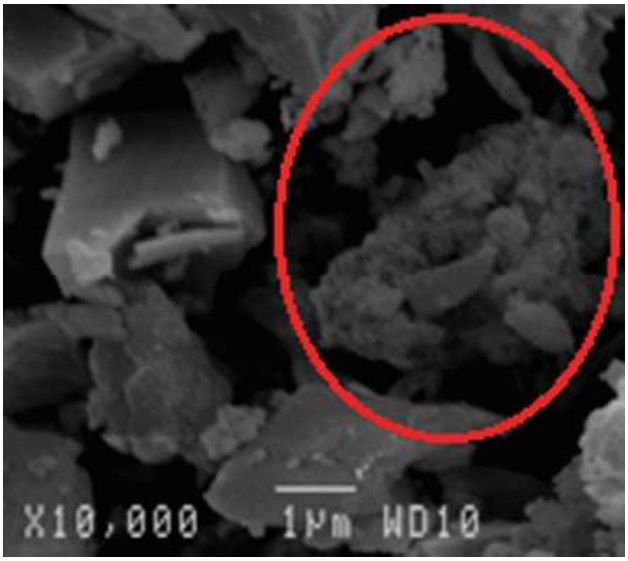

Fig. 26.6 Micrographs showing agglomeration of granite particles

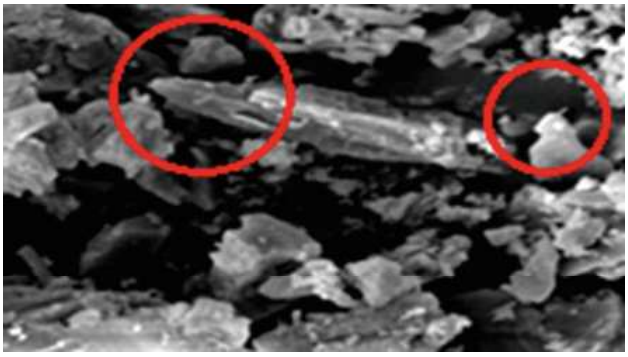

Fig. 26.7 Micrographs showing pointed nature of granite dust

Result and Discussion

Influence of Filler Loading on Hardness and Impact Strength of Polymer Composite

The hardness of FGM composites increases significantly as the weight percentage of granite powder increases, as shown in Fig. 26.8. The hardness of the FGM samples taken from five different sites was in the strict range (40.8 ± 0.6–53.75 ± 0.9) HV for (0–15)% of granite powder by weight. Maximum hardness was observed at 15% wt. of granite dust for FGM composites.

The evaluation of total absorbed energy during the fracture of the resulted epoxy composite is carried out by standard Charpy impact test. The outcome of Charpy test is shown in Fig. 26.9. It is worth noting that the impact strength of the fabricated material exhibits an increasing approach.

Table 26.3 L_{16} orthogonal design of experiment

S. No.	Speed (RPM)	Load (N)	Filler (%)	Distance (m)	DOE notations
1.	375	7.5	0	150	A11
2.	375	15	5	300	A12
3.	375	22.5	10	450	A13
4.	375	30	15	600	A14
5.	750	7.5	5	450	B11
6.	750	15	0	600	B12
7.	750	22.5	15	150	B13
8.	750	30	10	300	B14
9.	1125	7.5	10	600	C11
10.	1125	15	15	450	C12
11.	1125	22.5	0	300	C13
12.	1125	30	5	150	C14
13.	1500	7.5	15	300	D11
14.	1500	15	10	150	D12
15.	1500	22.5	5	600	D13
16.	1500	30	0	450	D14

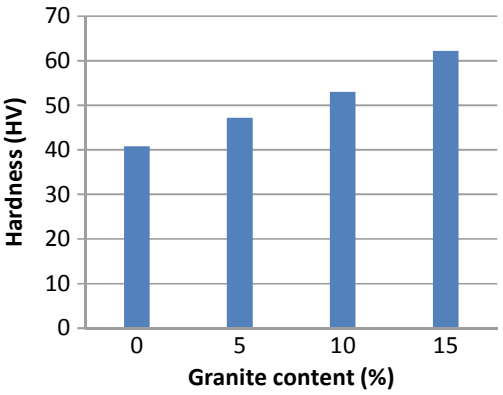

Fig. 26.8 Variation of hardness with granite content

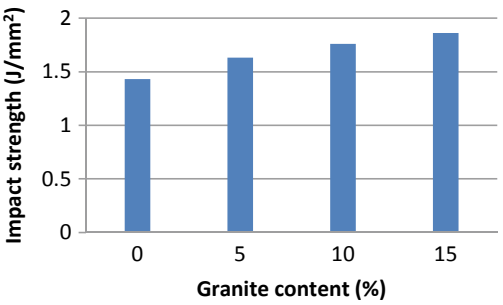

Fig. 26.9 Variation of Impact strength with Granite content

Adding filler material from 0 to 15 wt% increases the toughness potential of the material. However, the results were acquired successfully in the range ($1.43 \pm 0.006 - 1.86 \pm 0.003$) J/mm^2 for granite dust content.

Wear Analysis

The aggregate signal-to-noise ratio (SN ratio) of the wear rate of the FGM composite was found to be 43.898 dB. The wear result of fabricated composite materials is converted into signal to noise ratio. For smaller specific wear rate, the function ''less is better" is used as presented in equation below.

$$\frac{S}{N} = -10 \log\left[\frac{1}{n}\left(\sum y^2\right)\right]$$

where n is the number of observations and y is the data observed.

The wear analysis results are evaluated using the formation of Analysis Programming Minitab 18. Examination of the output revealed that A4, B3, C4 and D2 factor combination gives least wear rate (Fig. 26.10). Table 26.4 indicates the specific wear ratios of FGM (W). It can be seen that FGM alloys with granite dust content exhibit the highest wear resistance. If the appropriate testing technique is followed, the test produces enhanced wear rates.

Effect of Applied Load

The effect of various normal loads on the wear rate of reinforced specimens at fixed parameters, such as a sliding velocity of 143.25 rpm (0.75 m/s) and a sliding distance of 750 m is shown in Fig. 26.11. The wear rate of all samples increases with an increase in normal load. This is due to the fact that increased friction at a higher load leads to an increase in deboning and cracking of the specimens. It is also observed that under all test conditions, the rate of specific wear decreases with the addition of granite powder to 15 wt%.

The specific wear is directly proportional to the normal load, this is clearly visible when we infer from Fig. 26.11, and the reason for this behavior is relative as the normal load increases, there is a significant increase in the frictional thrust which in turn increases the area of friction. This leads to more weight loss and ultimately increases in wear.

Effect of Sliding Velocity

Figure 26.12 shows the influence of sliding velocity on the wear behavior of the epoxy matrix sample and reinforced by different weight fractions of granite (5, 10, 15%) at constant specification like applied load of 55 N and a sliding distance of 750 m. It can be seen that the wear rate of the composite decreases with increasing slip velocity, in contrast to the increase in load, and the weakest wear resistance is observed for the unreinforced epoxy matrix sample. It is also clear that wear rate

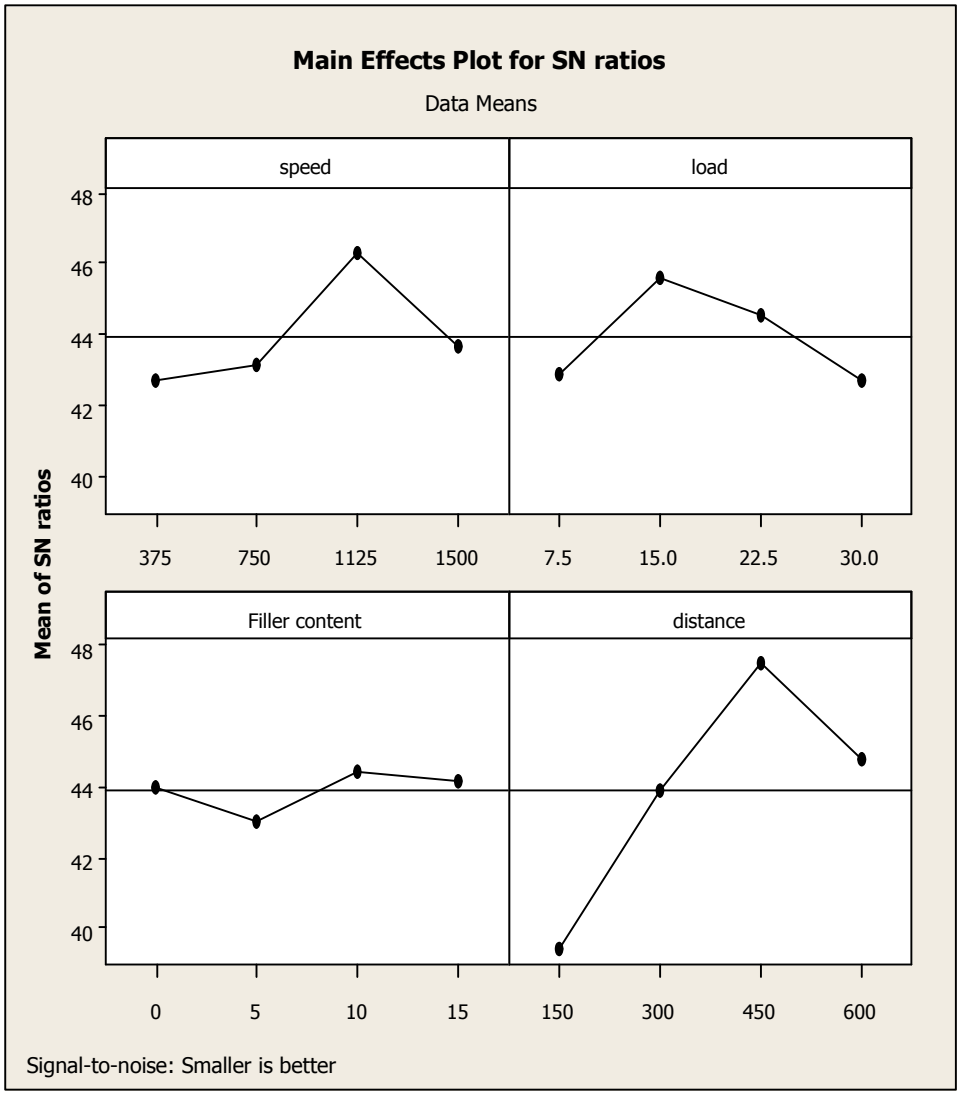

Fig. 26.10 Effect of control factors on wear rate of FGM composite

shows a declining trend under all test conditions with an increase in granite content, and the highest wear resistance is observed at 15% by weight of granite powder. Compared with the matrix, the abrasion resistance of the reinforced composites is higher due to the fact that granite particles impart additional strength to the epoxy composites and as a result shows excellent wear resistance.

Effect of Sliding Distance

Figure 26.13 shows the estimated wear rate for different sliding distances under test conditions. The graph illustrates the change in wear rate with sliding distance under a normal load of 55 N and sliding velocity of 143.25 RPM (0.75 m/s).

Table 26.4 Experimental design using L_{16} orthogonal array

S. No.	DOE notations	Sliding wear (W)	S/N ratio
1.	A11	1.57E−02	36.07095
2.	A12	6.76E−03	43.40107
3.	A13	4.98E−03	46.05541
4.	A14	5.62E−03	45.00527
5.	B11	4.38E−03	47.17052
6.	B12	6.06E−03	44.35055
7.	B13	1.06E−02	39.46933
8.	B14	8.64E−03	41.26973
9.	C11	4.68E−03	46.59508
10.	C12	2.96E−03	50.57417
11.	C13	3.41E−03	49.34491
12.	C14	1.20E−02	38.43086
13.	D11	8.32E−03	41.59753
14.	D12	6.43E−03	43.83578
15.	D13	6.94E−03	43.17281
16.	D14	4.96E−03	46.09037

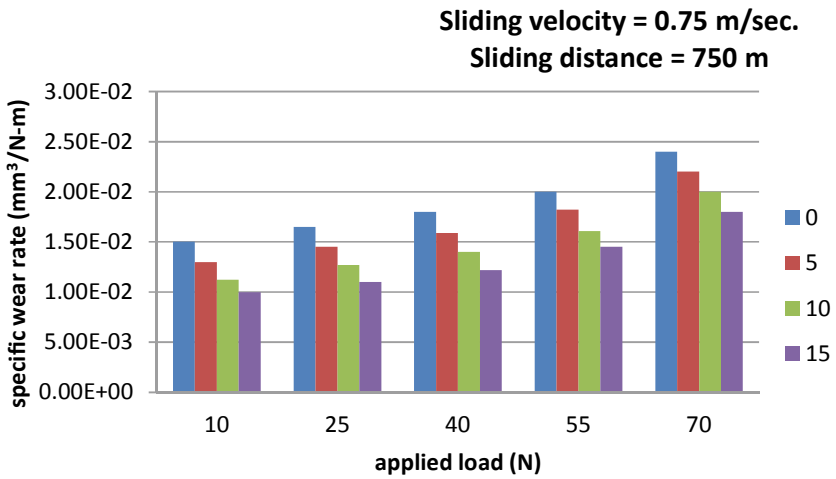

Fig. 26.11 Impact of load on wear rate with Granite content

All reinforced epoxy composites show improved wear resistance compared with matrix materials. It was observed that the wear rate increased with sliding distance for all samples. This may be due to the distinction of irregularities from the sample surface as shown in Fig. 26.14. It was also observed that the composites reinforced with 15 wt% granite powder showed minimal wear rates under all test conditions.

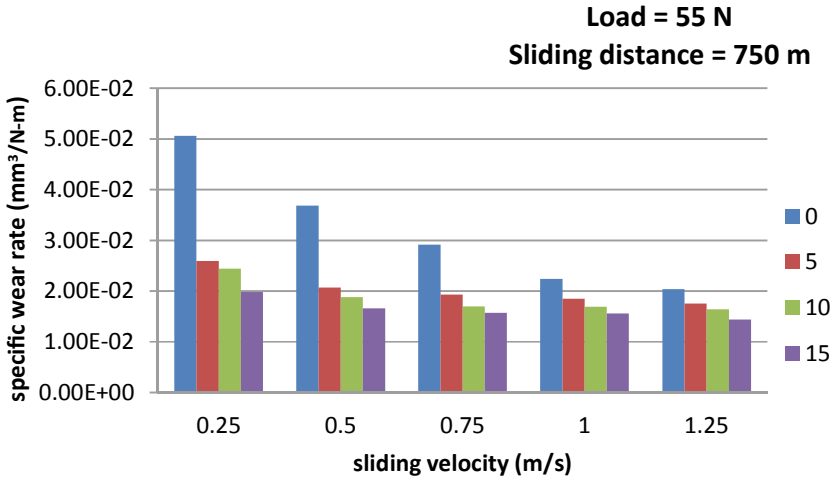

Fig. 26.12 Impact of sliding velocity on wear rate with Granite

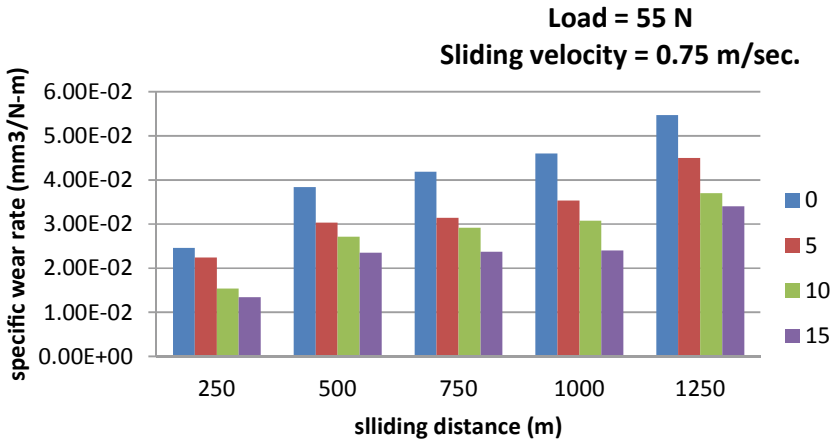

Fig. 26.13 Impact of sliding distance on wear rate with Granite

Fig. 26.14 Worn out surface irregularity of specimen

This again shows that the addition of fillers can improve the wear resistance of composites.

Conclusion

In the present investigation, graded granite dust reinforced epoxy composites are prepared by sustainable utilization of stone industry waste and their effect on the mechanical and wear performance is examined.

1. The hardness is increased with increment of granite filler into base matrix. The maximum hardness is 62.5 HV for 15 wt% granite reinforced FGM and minimum hardness is 40.3 HV for virgin FGM.
2. The impact strength is increased with increment of granite filler into base matrix. The maximum Impact strength is 1.86 J/mm^2 for 15 wt% granite reinforced FGM and minimum impact strength is 1.43 J/mm^2 for virgin FGM.
3. Granite powder electron microscope scanning was analyzed under different amplitude conditions.
4. The aggregate for signal-to-noise ratio (SN ratio) of wear rate for FGM composite is established to be 43.898 db.
5. The optimum levels of control factors are 1500 rpm, 22.5 N, 15 wt% and 300 m.
6. These results are mainly with correspondence to the above given reinforcements, it can be further inferred from the references that high granite dust content (i.e., 30–50%) will lead to excellent enhancement in wear characteristics of the fabricated composites.

References

1. Naebe M, Shirvanimoghaddam K (2016) Functionally graded materials: a review of fabrication and properties. Appl Mater Today 5:223–245
2. Shinohara Y (2013) Functionally graded materials. In: Somiya S (ed) Handbook of advanced ceramics. Academic Press, Oxford, pp 1179–1187
3. Li J, Peng X, Yang Y, Xu J, Wang P, Hong B, Jin D, Jin H, Wang X, Ge H (2018) A novel magnetic-field-driving method for fabricating Ni/epoxy resin functionally graded materials. Mater Lett 222:70–73
4. Zhang Y, Wang J (2017) Fabrication of functionally graded porous polymer structures using thermal bonding lamination techniques. Proc Manufact 10:866–875
5. Hassanin H, Jiang K (2018) Microfabrication of components based on functionally graded materials. Adv Ceram Matrix Compos 697–709
6. Rezapoor M, Razavi M, Zakeri M, Rahimipour MR, Nikzad L (2018) Fabrication of functionally graded Fe-TiC wear resistant coating on CK45 steel substrate byplasma spray and evaluation of mechanical properties. Ceram Int 44:22378–22386
7. Salcedo E, Baek D, Berndt A, Ryu JE (2018) Simulation and validation of three dimension functionally graded materials by material jetting. Addit Manufact 22:351–359

8. Gupta A, Talha M (2015) Recent development in modeling and analysis of functionally graded materials and structures. Prog Aerosp Sci 79:1–14
9. Polajnar M, Kalin M, Thorbjornsson I, Thorgrimsson JT, Botor-Probierz A (2017) Friction and wear performance of functionally graded ductile iron for brake pads. Wear 382–383:85–94
10. Chaubey AK, Gupta R, Kumar R, Verma B, Kanpara S, Bathula S, Khirwadkar SS, Dhar A (2018) Fabrication and characterization of W-Cu functionally graded material by spark plasma sintering process. Fusion Eng Des 135:24–30
11. Yusefi A, Parvin N, Mohammadi H (2018) W–Cu functionally graded material: low temperature fabrication and mechanical characterization. J Phys Chem Solids 115:26–35
12. Shen WP, Li Q, Chang K, Zhou ZJ, Ge CC (2007) Manufacturing and testing W/Cu functionally graded material mock-ups for plasma facing components. J Nucl Mater 367–370:1449–1452
13. Anigol NB, Pol AS (2015) Study of Effect of various fillers on mechanical properties of carbon-epoxy composites. Int Res J Eng Technol (IRJET) 02:798–802
14. Kumar BN, Ramesh BT (2015) Development and characterization of epoxy resin based granite powder and glass fibre reinforced composite. Int J Mod Trends Eng Res (IJMTER) 02:49–60
15. Balakrishna SS, Girish H, Kumar GCM, Narendranath S (2016) Analysis on mechanical and dynamic behavior of granite epoxy composites with cast iron particulates as filler. Ind J Adv Chem Sci 122–126
16. Kulkarni HB, Mahamuni SS, Gaikwad PM, Pula MA, Mahamuni S, Bansode SH, Kulkarni AA, Shete YB, Nehatrao SA (2017) Enhanced mechanical properties of epoxy/graphite composites. Int J Adv Eng Res Stud 6:01–05
17. Kareem AA (2013) Mechanical properties of granite powder as filler for polycarbonate toughened epoxy resin. Int J Pharma Sci 3:254–257
18. Radhika N, Raghu R (2016) Development of functionally graded aluminium composites using centrifugal casting and influence of reinforcements on mechanical and wear properties. Trans Nonferrous Met Soc China 26:905–916
19. Jamian S, Ayob SN, Abidin MRZ, Nor NHM (2016) Fabrication of functionally graded natural fibre/epoxy cylinder using centrifugal casting method. ARPN J Eng Appl Sci 11:2327–2331
20. Piratelli-Filho A, Shimabukuro F (2008) Characterization of compression strength of granite epoxy composites using design of experiments. Mater Res 11:399–404
21. Gangil B, Kukshal V, Sharma A, Patnaik A, Kumar S (2019) Development of hybrid fiber reinforced functionally graded polymer composites formechanical and wear analysis. AIP Conf Proc 2057:1–8
22. Ramakrishna HV, Padma Priya S, Rai SK, Rajulu AV (2005) Tensile, impact, and chemical resistance properties of granite powder-epoxy composites. J Reinf Plast Compos 24:451–455
23. Srivastava VK, Shembekar PS (1990) Tensile and fracture properties of epoxy resin filled with flyash particles. J Mater Sci 25:3513–3516
24. Ramakrishna HV, Rai SK (2006) Utilization of granite powder as a filler for polybutylene terepthalate toughened epoxy resin. J Miner Mater Charact Eng 5:1–19
25. Ramakrishna HV, Rai SK (2006) Effect on the mechanical properties and water absorption of granite powder composites on toughening epoxy with unsaturated polyester and unsaturated polyester with epoxy resin. J Reinf Plast Compos 25:17–32
26. Ray S, Rout AK, Sahoo AK (2017) A study on tribological behavior of glass-epoxy composite filled with granite dust. IOP Conf Ser Mater Sci Eng 225:1–8
27. Pawar MJ, Patnaik A, Nagar R (2015) Experimental investigation and numerical simulation of granite powder filled polymer composites for wind turbine blade: a comparative analysis. Polym Compos 1–8
28. Pawar MJ, Patnaik A, Nagar R (2016) Mechanical and thermo-mechanical analysis based numerical simulation of granite powder filled polymer composites for wind turbine blade. Fib Polym 17:1078–1089
29. Abdalrazaq I, Soud WA, Abdullah OS (2013) Effects of different types of ceramic fillers on wear characteristics of glass fibers-epoxy composite. J Eng Dev 17

30. Gangil B, Kumar S (2017) comparative evaluation on mechanical properties of jute/bamboo-glass hybrid reinforced polyester composites. Asian J Sci Technol 08:5190–5194
31. Soni S, Rana RS, Singh B, Rana S (2018) Synthesis and characterization of epoxy based hybrid composite reinforced with glass fiber and milled carbon. Mater Today: Proc 5:4050–4058